Space–Time Extremes in Short-Crested Storm Seas

FRANCESCO FEDELE

School of Civil and Environmental Engineering, and School of Electrical and Computer Engineering, Georgia Institute of Technology, Atlanta, Georgia

(Manuscript received 29 September 2011, in final form 1 May 2012)

ABSTRACT

This study develops a stochastic approach to model short-crested stormy seas as random fields both in space and time. Defining a space–time extreme as the largest surface displacement over a given sea surface area during a storm, associated statistical properties are derived by means of the theory of Euler characteristics of random excursion sets in combination with the Equivalent Power Storm model. As a result, an analytical solution for the return period of space–time extremes is given. Subsequently, the relative validity of the new model and its predictions are explored by analyzing wave data retrieved from NOAA buoy 42003, located in the eastern part of the Gulf of Mexico, offshore Naples, Florida. The results indicate that, as the storm area increases under short-crested wave conditions, space–time extremes noticeably exceed the significant wave height of the most probable sea state in which they likely occur and that they also do not violate Stokes–Miche-type upper limits on wave heights.

1. Introduction

One of the key elements in the analysis of long-term predictions of extreme wave crest events is the probability of exceedance of the maximum crest height $C_{\max}$ observed at a point Q in time t during a storm. Following Borgman (1973), this probability can be expressed as

$$\Pr\{C_{\max} > z\} = 1 - \exp\left(\int_0^D \frac{\ln\{1 - P[z \mid H_s = h(t)]\}}{\overline{T}[h(t)]}\, dt\right), \tag{1}$$

where $h(t)$ is the time series of the significant wave height H_s recorded at Q, $\overline{T}(h)$ is the mean zero up-crossing period, D is the storm duration, and $P(z \mid H_s = h)$ is the exceedance probability of the crest height z in a sea state where $H_s = h$. This is described reasonably well by the Rayleigh law or the Tayfun model for linear or nonlinear waves, respectively (Tayfun 1986; Tayfun and Fedele 2007; Fedele 2008; Fedele and Tayfun 2009).

Borgman's formulation (1) is the starting point of various statistical methods developed for predicting occurrences of extreme events in stormy seas (Krogstad 1985; Prevosto et al. 2000; Boccotti 2000; Isaacson and Mackenzie 1981; Guedes Soares 1988; Goda 1999; Arena and Pavone 2006, 2009; Fedele and Arena 2010). These assume that the effects of the sea state observed during time intervals of the short-term scales of $T_s \sim$ 1–3 h can be accumulated to predict the wave conditions for the long-term scales of $T_l \sim$ years. One of the drawbacks of such stochastic analyses is that, in short-crested seas, surface time series gathered at a fixed point tend to underestimate the true actual wave surface maximum that can occur over a given region of area E_s around Q. A large crest observed in time at Q represents a maximum observed at that point, but it may not even be a local maximum in the actual crest segment of a three-dimensional (3D) wave group. The actual crest representing the global maximum occurs at another point located without or within E_s. Certainly, the elevation of the actual crest is always larger than that measured at Q. Thus, (1) underestimates the maximum wave surface height $\eta_{\max}$ attained over E_s, which is also not the highest crest height of the group, unless the area is large enough for all wave-group dynamics to develop fully. Indeed, $\eta_{\max}$ can also occur on the region's boundaries, and this is usually the case in areas of smaller size than the average size of wave groups. Thus, wave extremes should be modeled in both space and time as maxima of random fields rather than those of

Corresponding author address: Francesco Fedele, School of Electrical and Computer Engineering, Georgia Institute of Technology, 777 Atlantic Drive NW, Atlanta, GA 30332.
E-mail: fedele@gatech.edu

DOI: 10.1175/JPO-D-11-0179.1

random functions of time (Adler 1981, 2000; Piterbarg 1995; Adler and Taylor 2007). Because in 3D random fields it is not possible to define a wave easily or unambiguously, as is possible in time series, in this work we refer to a space–time extreme as the largest surface displacement $\eta_{\max}$ over a given sea surface area during a storm.

Note that the application of such advanced stochastic theories to realistic oceanic conditions has been limited because it requires the availability of wave surface data measurements collected both in space and time, in particular directional wave spectra (Baxevani and Richlik 2004). Only at large spatial scales, synthetic aperture radar (SAR) or interferometric SAR (INSAR) remote sensing provides sufficient resolution for measuring waves longer than 100 m (see, e.g., Marom et al. 1990; Marom et al. 1991; Dankert et al. 2003). However, it is insufficient to correctly estimate spectral properties at smaller scales. At such scales, up-to-date field measurements for estimating directional wave spectra are challenging or inaccurate even if a linear or two-dimensional (2D) wave probe-type arrays could be used, though expensive to install and maintain (Allender et al. 1989; O'Reilly et al. 1996). Recently, stereo video techniques have been proposed as an effective low-cost alternative for such precise measurements (Benetazzo 2006; Wanek and Wu 2006; Fedele et al. 2011a,b; Gallego et al. 2011; Bechle and Wu 2011; de Vries et al. 2011; Benetazzo et al. 2012). Indeed, a stereo camera view provides both spatial and-temporal data whose statistical content are richer than that of a time series retrieved from wave gauges. For example, Gallego et al. (2011) have estimated directional spectra by a variational variant of the Wave Acquisition Stereo System (WASS) proposed by Benetazzo (2006). Further, WASS was used by Fedele et al. (2011a) to prove that in short-crested seas the maximum surface height over a given area is generally larger than that observed in time by point measurements (see also Forristall 2006). The fact that the spatial extremes are larger than those measured at a fixed point is not only because there are more waves in a spatial domain. The main reason is that fixed-point measurements cannot detect true extremes in short-crested seas. Theories due to Adler (1981) and Piterbarg (1995) follow from both reasons, especially from this essential difference between fixed-point versus true spatial picture. An extreme observed at a fixed probe in time in short-crested seas indicates that a wave crest section just propagated through the probe, and the probability that the actual extreme of that crest section coincides with the extreme observed in time is simply zero. It is only in long-crested seas that one can equate the extremes observed in time with the actual spatial extremes.

As pointed out by Baxevani and Richlik (2004), the occurrence of an extreme in a Gaussian field is analogous to that of a big wave that a surfer is in search of and always finds. Indeed, his likelihood to encounter a big wave increases if he moves around a large area instead of waiting to be hit by it. Indeed, if he spans a large area the chances to encounter the largest crest of a wave-group increase, in agreement with the findings of the recent European Union "MaxWave" project (Rosenthal and Lehner 2008).

In this work, the main focus is on characterizing the statistical properties of space–time extremes in short-crested sea states and their long-term predictions. The paper is structured as follows: First, the essential elements of the theory of Euler characteristics (EC; Adler 1981) are introduced. Then, their application is presented in the context of the Equivalent Power Storm (EPS) model of Fedele and Arena (2010). The statistical properties of space–time extremes are then derived. Further, the relative validity of the new model and its predictions are assessed by analyzing wave measurements and directional spectra retrieved from National Oceanic and Atmospheric Administration (NOAA) buoy 42003 (east Gulf of Mexico).

2. Euler characteristics and extremes

A significant result on the geometry of multidimensional random fields follows from the so-called Euler characteristics of their excursion sets (Adler 1981) and the relation to extremes. To keep the presentation simple, hereafter random fields in three dimensions or lower are considered, but the theory is valid in any dimensions (Adler and Taylor 2007). Consider a homogenous Gaussian wave field $\eta(x, y, t)$ over the bounded space–time volume Ω with zero mean and standard deviation σ (see Fig. 1). Here, homogeneity simply means that η is stationary in time and homogenous in space. Thus, the associated probability distributions at any points of the domain are the same and Gaussian, irrespective of the domain's size. Given a threshold z, define the excursion set $U_{\Omega,z}$ as that part of Ω within which η is above z: namely,

$$U_{\Omega,z} = \{(x, y, t) \in \Omega: \eta(x, y, t) > z\}. \qquad (2)$$

In 3D sets, the EC counts the number of connected volumetric components of the excursion set U, minus the number of holes that pass through it, plus the number of hollows inside. For 2D random fields instead, the EC counts the number of connected components minus the number of holes of the respective excursion set. In one-dimension (1D), the EC simply counts the number

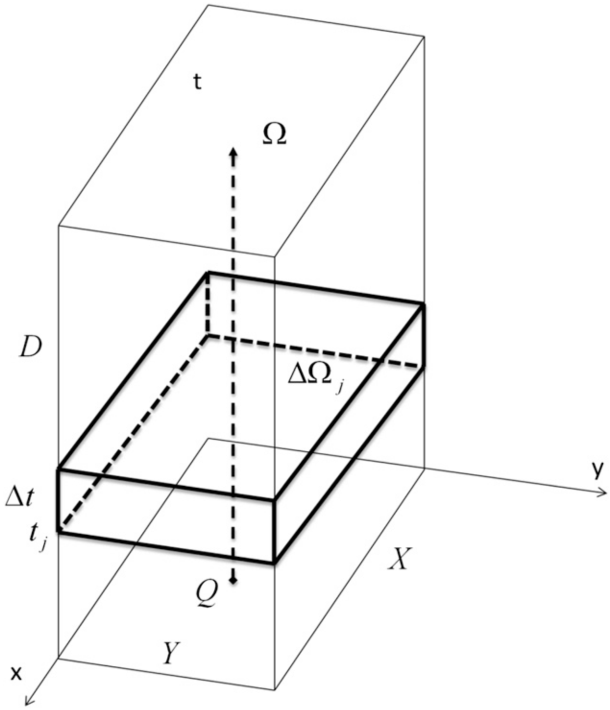

FIG. 1. Sketch illustrating definitions relevant to the space–time volume Ω.

of z upcrossings, thus providing their generalization to higher dimensions (Adler 1981).

Worsley (1996) presented various applications of EC theory to characterize the anomalies in the cosmic microwave background radiation, galactic topologies and cerebral activities in biomedical imaging. EC theory is also relevant to oceanic applications because Adler (1981) and Adler and Taylor (2007) have shown that the probability of exceedance $\Pr\{\eta_{\max} > z \mid \Omega\}$ that the global maximum $\eta_{\max}$ of η over Ω exceeds a threshold z depends on the domain size and it is well approximated by the expected EC of the excursion set $U_{\Omega,z}$, provided that the threshold is high. The expected EC approximation to the exceedance probability of $\eta_{\max}$ can be explained heuristically as follows. As z increases, the holes and hollows in the excursion set $U_{\Omega,z}$ disappear until each of its connected components includes just one local maximum of η, and the EC counts the number of local maxima. For very large thresholds, the EC equals 1 if the global maximum exceeds the threshold and 0 otherwise. Thus, $\mathrm{EC}(U_{\Omega,z})$ of large excursion sets is a binary random variable with states 0 and 1 and, for $z \gg \sigma$,

$$\Pr\{\eta_{\max} > z \mid \Omega\} = \Pr\{\mathrm{EC}(U_{\Omega,z}) = 1\} = \langle \mathrm{EC}(U_{\Omega,z}) \rangle, \tag{3}$$

where angled brackets denote expectation. This heuristic identity has been proved rigorously to hold up to an error that is in general exponentially smaller than any of the terms of the expected EC approximation (Taylor et al. 2005): namely,

$$\Pr\{\eta_{\max} > z \mid \Omega\} = \langle \mathrm{EC}(U_{\Omega,z}) \rangle + O\{\exp[-u^2(1+\chi)/2]\}, \tag{4}$$

where $u = z/\sigma \gg 1$ and the constant $\chi > 0$. Piterbarg (1995) also derived an asymptotic expansion of the probability in (3) for large Gaussian maxima via generalized Rice formulas (Rice 1944, 1945) valid for higher dimensions. In the following, we will first apply the preceding results to homogenous 3D Gaussian fields and then consider nonstationary space–time extremes observed during a sea storm.

a. Extremes of Gaussian fields

Consider the Gaussian field $\eta(x, y, t)$ homogenous over the space–time volume Ω of size XYD (see Fig. 1). Drawing upon Adler and Taylor (2007), define

$$M_3(D, X, Y \mid H_s) = 2\pi \frac{D}{\overline{T}} \frac{XY}{\overline{L}_x \overline{L}_y} \alpha_{xyt} \tag{5}$$

as the average number of 3D waves within Ω. Here, $\overline{T}$ is the mean wave period and $\overline{L}_x$ and $\overline{L}_y$ are the mean wave lengths along x and y, respectively. These, as well as the parameter α_{xyt}, are all estimated from the moments of the directional spectrum of η (see appendix A). The probability that one of the 3D waves exceeds the threshold z is given by

$$P_V(z \mid H_s) = [16(z/H_s)^2 - 1]P(z \mid H_s), \tag{6}$$

where

$$P(z \mid H_s) = \exp\left(-8\frac{z^2}{H_s^2}\right) \tag{7}$$

is the Rayleigh law.

If Ω is not large, then the threshold z can also be exceeded on the boundary surface $S = \partial\Omega$ with probability

$$P_S(z \mid H_s) = 4(z/H_s)P(z \mid H_s), \tag{8}$$

by one of the 2D waves. The average number of such occurrences is given by

$$M_2(D, X, Y \mid H_s) = M_{2,v} + M_{2,h}, \tag{9a}$$

where

$$M_{2,v} = \sqrt{2\pi} D \left(\frac{X}{\overline{T}\,\overline{L_x}} \sqrt{1-\alpha_{xt}^2} + \frac{Y}{\overline{T}\,\overline{L_y}} \sqrt{1-\alpha_{yt}^2} \right) \quad \text{and} \tag{9b}$$

$$M_{2,h} = \sqrt{2\pi}\, \frac{XY}{\overline{L_x}\,\overline{L_y}} \sqrt{1-\alpha_{xy}^2}. \tag{9c}$$

Here, $M_{2,v}$ ($M_{2,h}$) is the average number of 2D waves that occur on the vertical (horizontal) faces of $\partial\Omega$ and the parameters α_{xt}, α_{yt}, and α_{xy} also depend upon the directional spectrum (see appendix A).

The threshold z can also be exceeded along the perimeter $P = \partial S$ of the surface S. In this case, the number of such occurrences follows the Rayleigh law of (7). The average number of 1D waves that exceed u is given by

$$M_1(D, X, Y \mid H_s) = \frac{D}{\overline{T}} + \frac{X}{\overline{L_x}} + \frac{Y}{\overline{L_y}}. \tag{10}$$

There is no clear geometric criterion, such as that of zero upcrossings for 1D waves, for defining 2D or 3D waves. In simple terms, this can be thought as one of the space–time cells in which the map of the wave surface $\eta(x, y, t)$ can be portioned within a given volume or area.

For large thresholds $z \gg \sigma$, the probability of exceedance of the absolute maximum $\eta_{\max}$ of the wave surface η over Ω is given by

$$\Pr\{\eta_{\max} > z \mid \Omega\} = \Pr\{\eta_{\max} > z \mid V\} + \Pr\{\eta_{\max} > z \mid S\} + \Pr\{\eta_{\max} > z \mid P\}. \tag{11}$$

Here, each term on the right-hand side of the preceding equation denotes, from left to right, the probability that $\eta_{\max}$ is exceeded over the interior volume V of Ω, its surface S, or the perimeter P, respectively. The three terms can be derived as follows: The probability that $\eta_{\max}$ does not exceed z in V is equal to the probability that all the 3D waves in V have amplitudes less than or equal to z. If one assume the stochastic independence among waves (which holds for large z), then the first term in (11) can be expressed as

$$\Pr\{\eta_{\max} > z \mid V\} = 1 - \Pr\{\eta_{\max} \le z \mid V\} = 1 - [1 - P_V(z \mid H_s)]^{M_3} \tag{12}$$

and similarly for the other two terms: that is,

$$\Pr\{\eta_{\max} > z \mid S\} = 1 - \Pr\{\eta_{\max} \le z \mid S\} = 1 - [1 - P_S(z \mid H_s)]^{M_2} \tag{13}$$

and

$$\Pr\{\eta_{\max} > z \mid P\} = 1 - \Pr\{\eta_{\max} \le z \mid P\} = 1 - [1 - P(z \mid H_s)]^{M_1}. \tag{14}$$

For $z \gg \sigma$, the preceding will lead to

$$\Pr\{\eta_{\max} > z \mid \Omega\} \cong M_3 P_V(z \mid H_s) + M_2 P_S(z \mid H_s) + M_1 P(z \mid H_s), \tag{15}$$

in agreement with Adler and Taylor (2007).

b. *Scale dimension of extremes*

A statistical indicator of the geometry of space–time extremes in the volume Ω can be defined as (see appendix B)

$$\beta = 3 - \frac{4M_2\zeta_0 + 2M_1}{16M_3\zeta_0^2 + 4M_2\zeta_0 + M_1}, \tag{16}$$

where ζ_0 relates to the expected maximum surface height $\eta_{\max}$. The parameter β represents a scale dimension of waves: that is, the relative scale of a space–time wave with respect to the volume's size. From (16), it is easily seen that $1 \le \beta \le 3$. In particular, if $\beta = 3$, wave extremes are fully 3D and they are expected to occur within the volume V away from the boundaries. For $2 < \beta < 3$, extremes intersect also the lateral surface of V. The limiting case of $\beta = 2$ is attained when one of the three sides D, X, or Y is null: for example, $D = 0$. In this case, the extreme can occur within an area $E_s = XY$ and it is 2D. When the area's boundaries are touched by the extreme, then $1 < \beta \le 2$. The limiting case of 1D extremes ($\beta = 1$) occurs when the area E_s collapses to a line ($X = 0$ or $Y = 0$). As an example, Fig. 2 shows the wave dimension β computed for each hourly sea state of the H_s sequence recorded during the period 2007–09 by NOAA buoy 42003, moored off the east Gulf, for $D = 1$ h and squared $E_s = 100^2$ m^2. Clearly, in milder or low sea states, extremes are quasi 3D because mean wavelengths (~30 m) and periods (~3 s) are much smaller than the lateral length L and duration D, respectively. As the intensity of the sea state increases, so do both the associated mean wavelengths (up to ~190 m) and periods (up to ~12 s) and the wave dimension reduces; at the highest sea states, β is roughly 2.6 and waves appear more long crested. However,

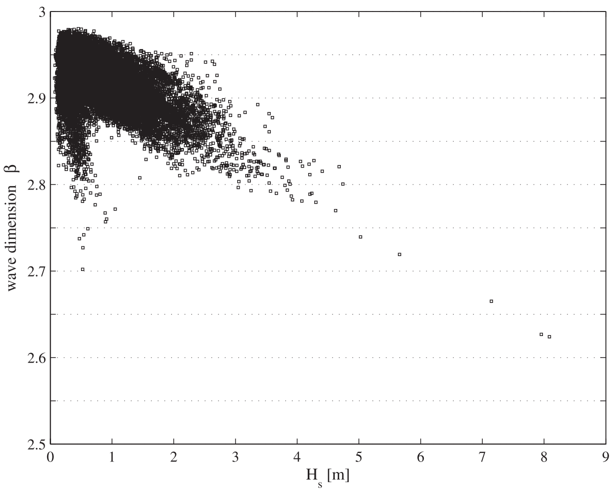

FIG. 2. Wave dimension β of each hourly sea state of the H_s sequence recorded by NOAA buoy 42003 during 2007–09 ($D = 1$ h and $X = Y = 100$ m).

their sea states are broadbanded and modulational effects are negligible. In this case, extremes are expected to occur on the surfaces X–T or Y–T of the volume V.

In the following sections, (15) is extended for a random wave field η homogenous in space but nonstationary in time, thus providing a means of predicting the maximum value of η over an area during a storm under more realistic conditions. This also leads to a generalization of the Borgman model (1) for predicting space–time extremes in storm seas with dominant second-order nonlinearities. As discussed above, the eventual application of such an approach requires spatial data, specifically directional spectra that can be estimated, for example via noninvasive stereo imaging techniques (Benetazzo 2006; Gallego et al. 2011; Fedele et al. 2011a) or via SAR/INSAR remote sensing (see, e.g., Marom et al. 1990; Marom et al. 1991; Dankert et al. 2003).

c. Space–time extremes during storms

Consider the space–time volume Ω of Fig. 1, and regard η as the wave surface generated by an actual storm passing through the area $E_s = XY$ during a time interval D. Assuming that η is spatially homogenous over the area but nonstationary in time, partition D into $J = D/\Delta t$ time intervals each centered at $t = t_j$, as shown in Fig. 1. Next, assume that η is locally or piecewise stationary in any time interval $[t_j, t_j + \Delta t]$, with Δt usually equal to 1 h or so. The sea storm is then defined as a sequence of 3D stochastically independent Δt sea states $\Delta\Omega_j$ with piecewise time-varying mean period $\overline{T}(t)$ and wavelengths $\overline{L}_x(t)$ and $\overline{L}_y(t)$. Such parameters can be estimated from the directional spectrum (see appendix A). The surface ΔS_j of $\Delta\Omega_j$ consists of four vertical faces aligned along the t axis and surrounding the interior ΔV_j. The perimeter $\partial\Delta S_j$ consists of four vertical segments, each of length Δt. With this setting in mind, the volume Ω is partitioned in disjoint subsets $\Omega = S_b \cup S_L \cup V \cup S_u$, where S_u and S_b are the upper and bottom surface areas of Ω at $t = 0$ and D, respectively, and the lateral surface S_L and interior volume V are given by

$$S_L = \bigcup_{j=1,J} \Delta S_j, \quad V = \bigcup_{j=1,J} \Delta V_j. \tag{17}$$

The exceedance probability of the global maximum $\eta_{\max}$ of η over Ω can then be expressed as

$$\begin{aligned}\Pr\{\eta_{\max} > z \mid \Omega\} = 1 - \Pr\{&(\eta_{\max} \le z \mid V) \\ &\cap (\eta_{\max} \le z \mid S_L) \cap (\eta_{\max} \le z \mid \partial S_L) \\ &\cap (\eta_{\max} \le z \mid S_b) \cap (\eta_{\max} \le z \mid S_u)\},\end{aligned} \tag{18}$$

where ∂S_L is the perimeter of S_L. Assuming stochastic independence, as $\Delta t \to 0$ or $J \to \infty$, (18) yields the extended Borgman exceedance probability to space–time (see appendix C for derivation),

$$P(\eta_{\max} \mid E_s > z) = 1 - \exp\left[\int_0^D (P_1 + P_2 + P_3)\, dt\right], \tag{19}$$

where

$$P_1(z \mid H_s = h) = \frac{\ln\{1 - P[z_1 \mid H_s = h(t)]\}}{\overline{T}[h(t)]}, \tag{20}$$

$$P_2(z \mid H_s = h) = N_S \frac{\ln\{1 - P_S[z_1 \mid H_s = h(t)]\}}{\overline{T}[h(t)]}, \quad \text{and} \tag{21}$$

$$P_3(z \mid H_s = h) = N_V \frac{\ln\{1 - P_V[z_1 \mid H_s = h(t)]\}}{\overline{T}[h(t)]}, \tag{22}$$

where the coefficients N_S and N_V are given in appendix A. Here, to account for second-order nonlinearities, the linear amplitude z_1 is related to the nonlinear amplitude z via the quadratic equation $z = z_1 + \mu z_1^2/2\sigma$ (Tayfun 1980, 1986; Fedele and Tayfun 2009), where $\mu = \lambda_3/3$ represents an integral measure of steepness dependent on the skewness coefficient λ_3 of η.

Note that (19) is a normalized probability measure because $P(\eta_{\max} \mid E_s > 0) = 1$. As $E_s \to 0$, it reduces to

$$P(\eta_{\max} > z) = 1 - \exp\left(\int_0^D P_1\, dt\right), \qquad (23)$$

which is the Borgman probability in (1) for the maximum wave crest $C_{\max}$ observed in time at point Q. The expected maximum $\overline{\eta}_{\max}$ of the actual storm follows by integrating (19) over z as

$$\overline{\eta}_{\max} = \int_0^\infty P(\eta_{\max} \mid E_s > z)\, dz. \qquad (24)$$

As $z \to \infty$, (19) tends asymptotically to

$$P(\eta_{\max} \mid E_s > z) \to -\int_0^D (P_1 + P_2 + P_3)\, dt, \qquad (25)$$

which is the extension of Adler's probability (15) to sea storms.

Note that the exceedance probability in (19) relies on the assumption of stochastic independence of large waves, which holds for weakly non-Gaussian fields dominated by second-order nonlinearities or short-crested seas considered in this work. Indeed, realizations of maxima typically occur at times and locations typically well separated to render them largely independent of one another in wind seas. Clearly, in long-crested sea states the areal effects are negligible and (19) reduces to the time Borgman formulation (1). However, in this case the wave surface is affected by nonlinear quasi-resonant interactions and fourth-order cumulants increase beyond the Gaussian threshold if the spectrum is narrow (see, e.g., Fedele et al. 2010). To account for such deviations, an obvious modification would be to simply replace in (1) the Rayleigh/Tayfun distribution with the Gram–Charlier (GC) type of models, such as those developed by Mori and Janssen (2006), Tayfun and Fedele (2007), or Fedele (2008). Indeed, GC models have been shown to describe the effects of quasi-resonant interactions on the wave statistics (see, e.g., Fedele et al. 2010). However, in such long-crested sea states individual waves are correlated (see, e.g., Janssen 2003) and (1), even with a GC model, loses its validity and yields conservative estimates as an upper bound. The space–time stochastic model proposed herein can be extended to smoothly bridge long- and short-crested conditions. This would require taking into account the correlation between neighboring waves, and it should depend upon the joint probability distribution of successive extremes (see, e.g., Fedele 2005). Such a model would be beneficial for estimating extreme waves in rapid development of long-crested sea states in time. Some work on marine accidents suggests that such conditions may occur (Tamura et al. 2009). The development of such a stochastic model is in progress and will be discussed elsewhere.

3. Prediction and properties of space–time extremes

In the following, (19) will be applied in the context of the EPS model of Fedele and Arena (2010) to predict the long-term statistics of space–time extremes: namely, the largest surface elevation $\eta_{\max}$ that can occur over the area E_s centered at point Q during a storm. To do so, consider a time interval τ during which $N(\tau)$ storms sweep through E_s, and assume that the time series of significant wave heights H_s at Q as well as the directional spectrum are given as measurements. Then, define a succession of storms where each storm, according to Boccotti (2000), is identified as a nonstationary sequence of sea states in which H_s exceeds 1.5 times the mean annual significant wave height at the site, and it does not fall below that threshold during an interval of time longer than 12 h (see also Arena 2004). Given a succession of storm events in time, each event is described as an EPS storm of duration b and peak amplitude a at, say, $t = t_0$. The significant wave height h varies in time t according to a power law $h(t) \sim |t - t_0|^\lambda$, where λ (>0) is a shape parameter (Fedele and Arena 2010). The EPS storm has sharp cusps for $0 < \lambda < 1$ and rounded peaks for $\lambda \geq 1$. For $\lambda = 1$, the ETS model of Boccotti with linear cusps is recovered (Boccotti 2000). It is then assumed that a and b are realizations of two random variables: for example, A and B, respectively. Then, the storm-peak probability density function (pdf) $p_A(a)$ is not fitted directly to the observed storm-peak data via ad hoc regressions, but it follows analytically by requiring that the average times spent by the equivalent and actual storm sequences above any threshold be identical: namely,

$$p_A(a) = \frac{\tau}{N(\tau)} \frac{a}{\overline{b}(a)} G(\lambda, a). \qquad (26)$$

Here, the function $G(\lambda, a)$ (see Appendix D) depends on the exceedance distribution of significant wave heights $P(h) = \Pr\{H_s > h\}$ and the conditional average duration $\overline{b}(a \mid E_s) = \overline{B \mid A = a}$, both of which are estimated via regression. In particular, a Weibull fit is adopted for $P(h)$ as

$$P(h) = \exp\left[-\left(\frac{h - h_l}{w}\right)^u\right], \qquad (27)$$

where u, w, and h_l are regression parameters (see Fedele and Arena 2010). As a consequence, the analytical form of the storm-peak density p_A is defined via (26). For example, for triangular storms ($\lambda = 1$),

$$p_A(a) \sim \frac{a}{\overline{b}(a)}\frac{d^2P}{da^2} = \frac{u}{w\overline{b}(a)}\left(\frac{a-h_l}{w}\right)^{u-1} \times\left[u\left(\frac{a-h_l}{w}\right)^{u}+u-1\right] \times\exp\left[-\left(\frac{a-h_l}{w}\right)^{u}\right], \quad (28)$$

and p_A depends upon the Weibull parameters and the conditional $\overline{b}(a)$. For comparison, both the generalized extreme value (GEV) and Gumbel (G) models are used to fit the observed storm-peak data. In particular, the GEV density and cumulative distribution function are given by

$$p_{\mathrm{GEV}}(a) = \frac{dP_{\mathrm{GEV}}}{da},$$
$$P_{\mathrm{GEV}}(a) = \Pr\{A \le a\} = \exp[-(1+k(a-\mu)/\sigma)^{-1/k}], \quad a \ge \mu - \sigma/k, \quad (29)$$

where (k, μ, σ) are the GEV parameters. For Gumbel,

$$p_G(a) = \frac{dP_G}{da},$$
$$P_G(a) = \Pr\{A \le a\} = \exp\{-\exp[-(a-\mu_G)/\sigma_G]\}, \quad a \ge 0, \quad (30)$$

where (μ_G, σ_G) are regression parameters. Note that GEV tends to G as $k \to 0$.

The conditional storm base is estimated as follows: For large z, the probability that $\eta_{\max} > z$ during an EPS storm is given by

$$P\{\eta_{\max} \mid E_s > z; a, b\} = 1 - \exp\left[\frac{b}{\lambda a}\int_0^a \frac{P_1(z\mid h)+P_2(z\mid h)+P_3(z\mid h)}{(1-h/a)^{1-1/\lambda}}\,dh\right]. \quad (31)$$

This follows from (19) specializing the significant wave height history $h(t)$ to that of the EPS storm (see Fedele and Arena 2010). As $E_s \to 0$, (31) reduces to the time-based Borgman probability (1) specialized to point estimates of the maximum crest height $C_{\max} = \eta_{\max}$ in EPS storms: namely,

$$P\{\eta_{\max} > z; a, b\} = 1 - \exp\left[\frac{b}{\lambda a}\int_0^a \frac{P_1(z\mid h)}{(1-h/a)^{1-1/\lambda}}\,dh\right]. \quad (32)$$

The expected maximum $\overline{\eta}_{\max}(E_s)$ of the EPS storm then follows by integration as in (24). For a given area E_s, the statistical equivalence between an actual storm and the associated EPS is achieved by requiring that a equal the actual maximum H_s in the storm, and b is chosen so that the expected maximum $\overline{\eta}_{\max}$ during the storm is the same as that of the EPS storm (Fedele and Arena 2010). Once the $\overline{\eta}_{\max}$ of the true storm is estimated from data by means of (19) and (24), a good approximation of b is given by imposing the exceedance probabilities of the actual and EPS storms to be equal at $z = \overline{\eta}_{\max}$: namely,

$$P\{\eta_{\max} \mid E_s > \overline{\eta}_{\max}; a, b\} = P(\eta_{\max} \mid E_s > \overline{\eta}_{\max}). \quad (33)$$

From this, b follows as

$$b(E_s, \lambda) = \lambda a \frac{\displaystyle\int_0^D (P_1+P_2+P_3)\,dt}{\displaystyle\int_0^a \frac{P_1+P_2+P_3}{(1-h/a)^{1-1/\lambda}}\,dh}, \quad \text{for} \quad z = \overline{\eta}_{\max}. \quad (34)$$

It is observed that b depends upon the storm shape, but it slightly changes with the area E_s as expected, because b and the storm-peak density p_A are unique temporal properties of the given location, as a result of the assumed spatial homogeneity. Thus, hereafter b is estimated as $b(E_s, \lambda) \approx b(0, \lambda)$, based on the Borgman time-based model (32). As an example, Fig. 3 (top) shows one of the largest observed actual storms and the associated EPS. In the same figure, the exceedance probability (32) of the maximum crest height expected in time at the buoy location is compared for both the actual and EPS storms.

Given λ, the conditional average $\overline{b}(a)$ at the buoy location is then described by

$$\overline{b}(a) = b_m \exp[s_m(a - a_0)], \quad (35)$$

where b_m, s_m, and a_0 are regression parameters (Boccotti 2000).

Note that the EPS model depends on the measured data only via the observed $P(h)$ and the density p_A is estimated by way of (26) for an arbitrary $\lambda > 0$. As a result, the EPS model is defined in a probabilistic setting, and no further data fitting is necessary for estimating extremes and associated statistics, which can be expressed explicitly as a function of p_A. Indeed, the return period $R(H_s > h)$ of an actual storm whose peak is greater than a given threshold h can be expressed as (Fedele and Arena 2010)

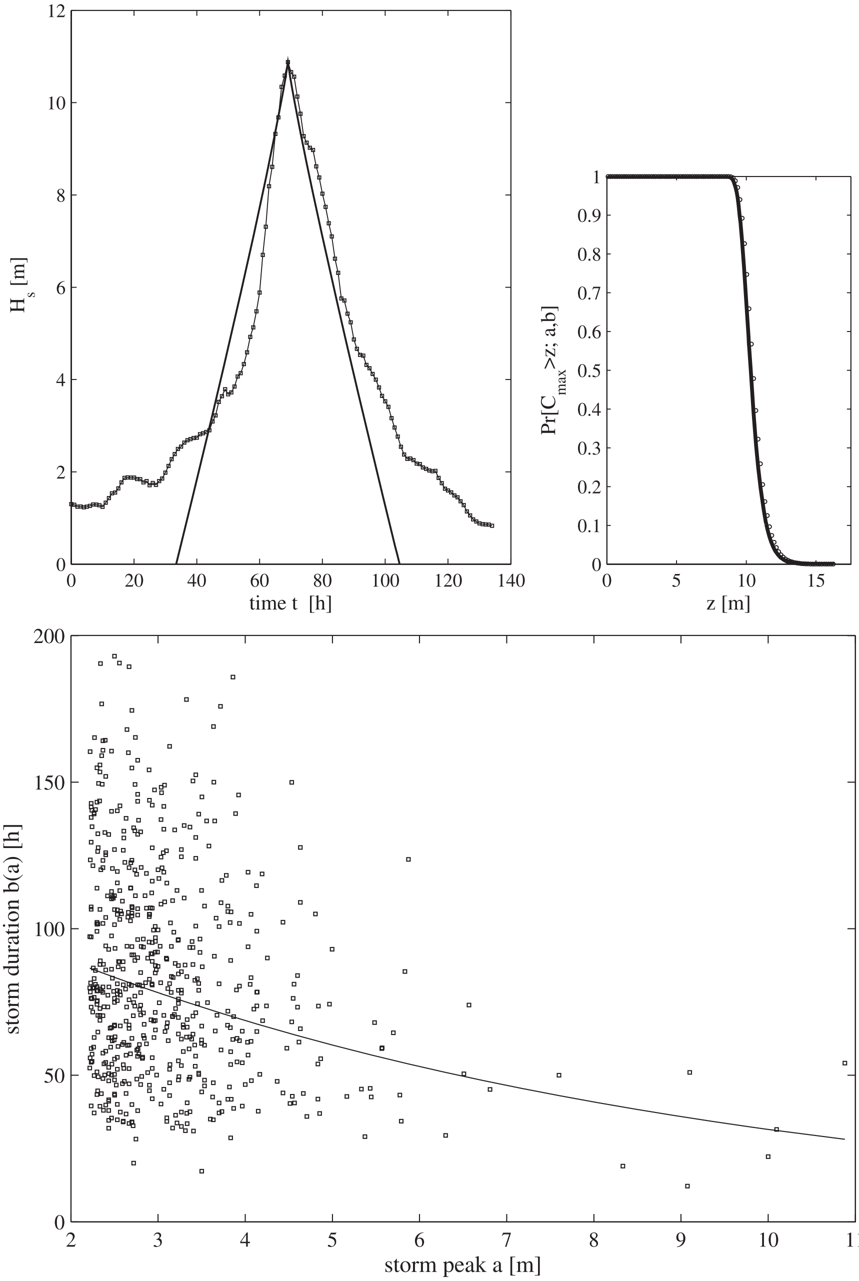

FIG. 3. NOAA buoy 42003: (top) shape and exceedance probability of the maximum time crest height $C_{\max}$ of the observed actual storm and the associated EPS storm and (bottom) duration of EPS storms and conditional base regression $\overline{b}(a)$ from Eq. (40) (regressions parameters $b_m = 86.5$ h, $s_m = -0.13$ m^{-1}, and $a_0 = 2.22$ m).

$$R(H_s > h) = \frac{\tau}{N(\tau)\int_h^{\infty} p_A(a)\,da}. \tag{36}$$

This can also be derived exploiting compound Poisson processes (Tayfun 1979).

The return period $R(\eta_{\max} \mid E_s > z)$ of an actual storm in which the maximum wave surface height exceeds z can be derived a follows: Consider the number $N_w(z \mid E_s)$ of equivalent storms where the maximum surface elevation over E_s during the storm is greater than z. Then, $R(\eta_{\max} \mid E_s > z)$ of an actual storm is defined as that of an equivalent storm whose global maximum $\eta_{\max}$ exceeds z. Thus,

$$R(\eta_{\max} \mid E_s > z) = \frac{\tau}{N_w(z \mid E_s)}, \tag{37}$$

where $N_w(z)$ can be explicitly formulated by following the same logical steps as in Fedele and Arena (2010). It is given by

$$N_w(z \mid E_s) = \frac{1}{\tau}\int_z^\infty p_A(a) P[(\eta_{\max} \mid E_s > z; a, \overline{b}(a)]\, da. \tag{38}$$

Using (38), (37) is simplified further to

$$R(\eta_{\max} \mid E_s > z) = \frac{1}{\displaystyle\int_z^\infty \frac{a}{\overline{b}(a)} G(\lambda, a) P[(\eta_{\max} \mid E_s > z; a, \overline{b}(a)]\, da}. \tag{39}$$

As $E_s \to 0$, this expression reduces to that for point measurements [i.e., $R(\eta_{\max} > z)$; see Arena and Pavone 2006] and thus yields the return period of a storm whose largest crest height exceeds z at a given location in time. Drawing upon Fedele and Arena (2010) and from probabilistic principles, one can also estimate the most probable value of the peak significant wave height A of the storm during which the maximum $\eta_{\max}$ exceeds a given threshold (e.g., z) over the area E_s. Indeed, given that $F = \{\eta_{\max} > z \mid E_s\}$, the conditional probability density function describing the relative frequency of occurrence of the extreme event in the equivalent storm whose peak intensity A is in $[a, a + da]$ is given by

$$p_{A|F}(a; z) = \frac{p_A(a) P(\eta_{\max} \mid E_s = z; a, \overline{b}(a))}{\displaystyle\int_0^\infty p_A(a) P(\eta_{\max} \mid E_s = z; a, \overline{b}(a))\, da}. \tag{40}$$

The conditional mean $\mu_{A|F}(z, E_s)$ and standard deviation $\sigma_{A|F}(z, E_s)$ are both function of z and area E_s. If the coefficient of variation $\gamma = \sigma_{A|F}/\mu_{A|F} \ll 1$, then an exceptionally high surface elevation most likely occurs during a storm whose maximum significant wave height (i.e., the storm peak A) is very close to $\mu_{A|F}$. Most likely this is also the intensity of the sea state in which the expected extreme occurs. In the applications to follow, it will be shown that theoretical predictions such as these implied by the EPS models are approximately satisfied in actual storm data. Moreover, to compare the EPS predictions with those based on GEV and G models, the return periods $R(H_s > h)$ and $R(\eta_{\max} \mid E_s > z)$ will be also estimated replacing p_A with p_{GEV} and p_G, which follow from the storm-peak data via (29) and (30).

4. Long-term extremes in the east Gulf

Hereafter, the space–time EPS model will be applied to elaborate some wave measurements retrieved by the NOAA buoy 42003 moored west of Naples, Florida, during 1976–2009. The data indicates that the observed sea states at the buoy location are short crested in agreement with the analysis of Forristall (2007) (see also Forristall and Ewans 1998). Indeed, their angular spreading $\Delta\theta$, estimated as in O'Reilly et al. (1996), is in the range of [30°–60°]. The time series of long-term wave statistics for point measurements have been elaborated showing that the exceedance distribution $P(h)$ of significant wave heights is well represented by the Weibull law (27) with parameters u = 0.591, w = 0.201 m, and h_l = 0 m. Further, directional data available for the period 2000–09 are used to fit the wave parameters $\overline{T}$, $\overline{L}_x$, and $\overline{L}_y$ from the hourly measured directional spectra as

$$\overline{T} = \gamma_T \sqrt{4H_s/g}, \quad \overline{L}_x = \gamma_X g \overline{T}^2, \quad \overline{L}_y = \gamma_y g \overline{T}^2, \tag{41}$$

where $\gamma_T = 2.42$, $\gamma_X = 0.171$, and $\gamma_y = 0.172$. From the analysis of the estimated directional spectra of the hourly sea states, the spectral parameters α_{xt}, α_{xt}, and α_{xy} are on average very small and can be set equal to zero as conservative estimates, whereas $\alpha_{xyt} \sim 0.7$ as an average. For the data at hand, quasi-triangular storms are optimal ($\lambda \sim 0.9$) (see Fig. 3, top), and the conditional base $\overline{b}(a)$ can be estimated from a sequence of $N(\tau) = 627$ storms: it is reported in Fig. 3 (bottom).

Given $P(h)$ and $\overline{b}(a)$, one can now compute the pdf $p_A(a)$ of the storm-peak intensity A from (26) and predict the return period $R(H_s > h)$ from (36) for the NOAA buoy 42003. Figure 4 illustrates such predictions labeled as EPS. For comparison, the predictions based on the estimates of p_A directly from the observed storm-peak data using GEV and Gumbel models [cf. Eqs. (29) and (30)] are also reported. Note that EPS and G yield similar predictions, whereas GEV leads to overestimation at large R. The associated return period $R(\eta_{\max} \mid E_s > z)$ of the largest surface height over a square area $E_s = L^2$, with $L = 10^3$ m, is computed from (39) and shown in Fig. 5 for EPS, GEV, and Gumbel. For comparisons, the associated time predictions of the return period $R(\eta_{\max} > z)$ $(E_s = 0)$ are also shown. Clearly, the expected wave height $\eta_{\max}$ attained over E_s is larger than that expected at given point in time. Further, as the area increases the predictions tend to deviate

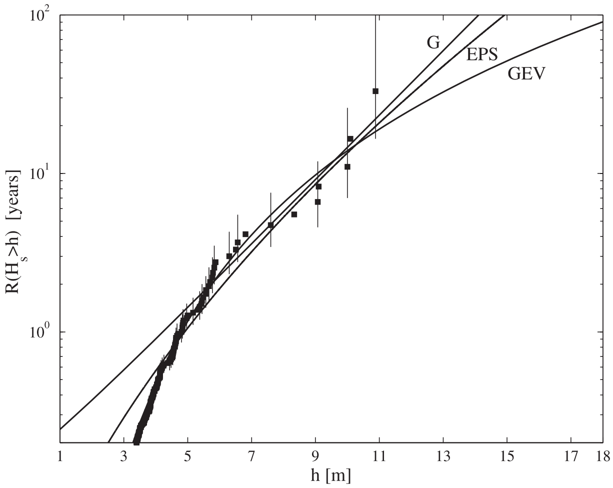

FIG. 4. NOAA buoy 42003: predicted return period $R(H_s > h)$ estimated with G, GEV, and EPS models (G parameters: $\mu_G = -2.007$ m and $\sigma_G = 2.135$ m; GEV parameters: $\mu = 2.656$ m, $\sigma = 0.422$ m, and $k = 0.353$; Weibull parameters for EPS: $u = 0.591$, $w = 0.201$ m, and $h_l = 0$).

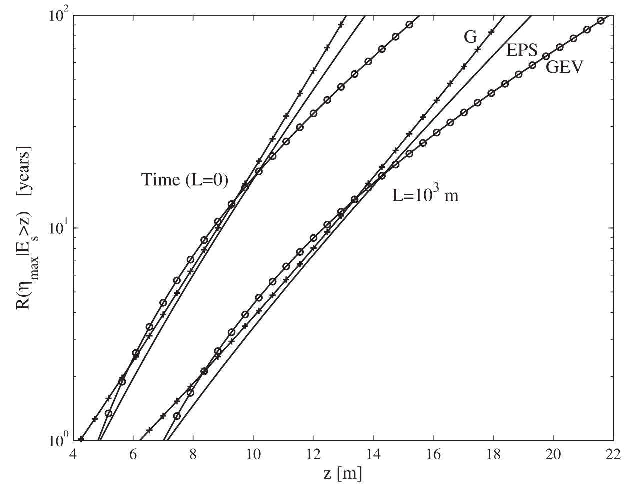

FIG. 5. NOAA buoy 42003: predicted return periods $R(\eta_{\max} > z)$ (labeled as time) and $R(\eta_{\max} \mid E_s > z)$ over the area $E_s = L^2$ ($L = 10^3$ m) estimated with G, GEV, and EPS models (regression parameters as in Fig. 4).

from the time Borgman counterpart as shown in Fig. 6 (right), which reports the EPS predictions of $\eta_{\max}$ as function of R over increasing areas with $L = 10^2$, 10^3, and 10^4 m, respectively. Over such large areas, the wave dimension β is expected to be roughly 3 (see Fig. 2 for the case $L = 100$ m). Thus, drawing upon Boccotti (2000), most likely $\eta_{\max}$ is the highest crest height of the central wave of a group that focuses within the area. An estimate of the associated steepness ε_h is needed to assess if the large crest violates the Stokes–Miche upper limit for breaking. To do so, given R we need an estimate of the most probable value $a_{\max}$ of the peak significant wave height A of the storm during which such maximum $\eta_{\max}$ exceeds z. This can be inferred using Eq. (40), which allows to predict the mean $\mu_{A|F}$ of the conditional pdf $p_{A|F}(a; z)$ of A given $F = \{\eta_{\max} > z \mid E_s = L^2\}$. The stability bands for such estimate proceed from the standard deviation $\sigma_{A|F}$. Figure 6 (middle) shows the associated ratio $\eta_{\max}/a_{\max}$ as function of R for the predictions in Fig. 6 (top). For the largest area considered ($L = 10^4$ m), this ratio increases to roughly 1.5–1.6, thus significantly exceeding the predictions at a given point in time (i.e., 0.9–1.1), in agreement with the stereo measurements of ocean waves (Fedele et al. 2011a). Given $a_{\max}$, the expected steepness can be expressed as $\varepsilon_h = k_h \eta_{\max}$, where the wavenumber k_h can be estimated in various ways. For example, one can extract its value from the actual wave profile if available. Equivalently, the theory of quasi determinism (Boccotti 1997a,b, 2000; Fedele and Tayfun 2009) suggests that a large crest at focusing tends to assume the same shape as the spatial covariance. Specifically, one can take the wavelength and thus the corresponding wavenumber value along the direction with the shortest zero-crossing wavelength (method 1). Alternatively, the period T_h of the largest wave can be estimated from the time covariance (Boccotti 2000), and k_h follows from the dispersion relation as $k_h = (2\pi/T_h)^2/g$ (method 2). For NOAA buoy 42003, $T_h \sim 1.26\overline{T} = 3.33\sqrt{4H_s/g}$ is a decent fit, especially for intense sea states. Figure 6 (bottom) reports both the expected steepness ε_h and the associated confidence intervals as function of R (estimates from the T_h fit). It is seen that the Stokes–Miche upper limit $\varepsilon_{\max} \sim 0.44$ (Stokes 1880; Michell 1893) is not violated by large waves (see also Tayfun 2008). This result clearly suggests that exceptional waves with $\eta_{\max}/a_{\max} > 1$ can occur over larger areas. However, a more critical analysis of the breaking conditions is required, but this goes beyond the scope of this paper.

Finally, to confirm the above long-term predictions the H_s sequence of hourly sea states recorded by NOAA buoy 42003 during the period 2007–09 has been analyzed. In particular, Fig. 7 (top) reports the short-term ($D = 1$ h) expected maximum surface height $\eta_{\max}/H_s$ attained over $E_s = XY$ ($X = Y = 10^3$ m) for each hourly sea state. The associated ε_h (Fig. 7, bottom) is also estimated directly from the directional spectrum using methods 1 and 2, with differences less than 2%. Clearly, extremes of intense sea states do not violate the Stokes–Miche upper limit in agreement with the long-term predictions of Fig. 6.

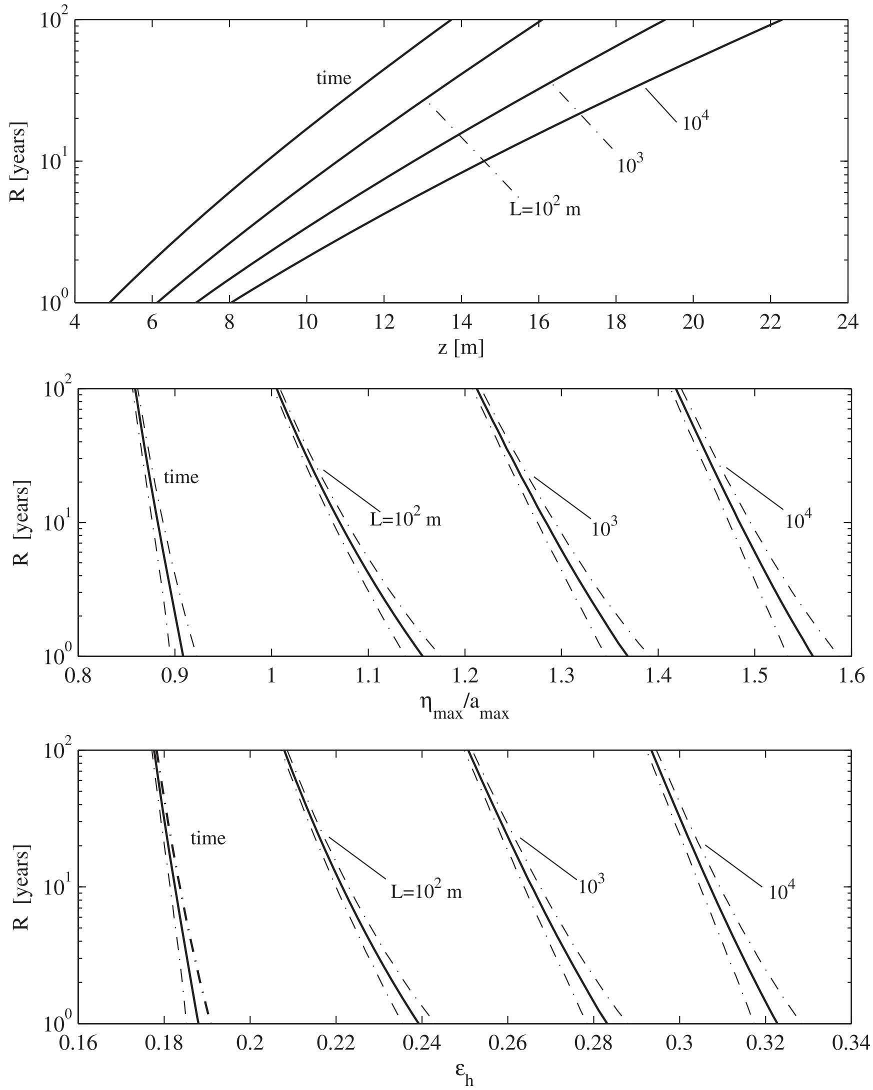

FIG. 6. NOAA buoy 42003: (top) predicted return period $R(\eta_{\max} \mid E_s > z)$ of the largest surface height $\eta_{\max}$ over increasing areas $E_s = L^2$ with $L = 0$ (time), 10^2, 10^3, and 10^4 m estimated with the EPS model (regression parameters as in Fig. 4); (middle) significant wave height $H_s = a(\eta_{\max})$ of the most probable sea state in which $\eta_{\max}$ occurs in terms of the ratio $\eta_{\max}/H_s$; and (bottom) steepness ε_h of the associated extreme wave.

5. Conclusions

The stochastic model developed herein extends the Borgman time-domain model (1) to space–time extremes and demonstrates the increased likelihood of large waves over a given area in short-crested seas (see also Baxevani and Richlik 2004). The proposed model was applied to several storms recorded by the NOAA buoy 42003. The results reveal that given a return period, the associated threshold z exceeded by the maximum surface height $\eta_{\max}$ over a given area is greater than that predicted by the Borgman time-domain model. In particular, for the largest area considered ($L = 10^4$ m), $\eta_{\max}$ exceeds 1.4 times the significant wave height $a_{\max}$ of the sea state where the maximum occurs, significantly exceeding the ratio $\eta_{\max}/a_{\max} \sim 0.9$–$1.1$ predicted from the Borgman model. These results are in agreement with those obtained from the recent stereo measurements by Fedele et al. (2011a). In intense sea states, if the area is large enough compared to the mean wavelength, a space–time extreme most likely coincides with the crest of a focusing wave group that passes through the area. Further, estimates of the steepness of such large crests suggest that they do not violate the Stokes–Miche upper limit.

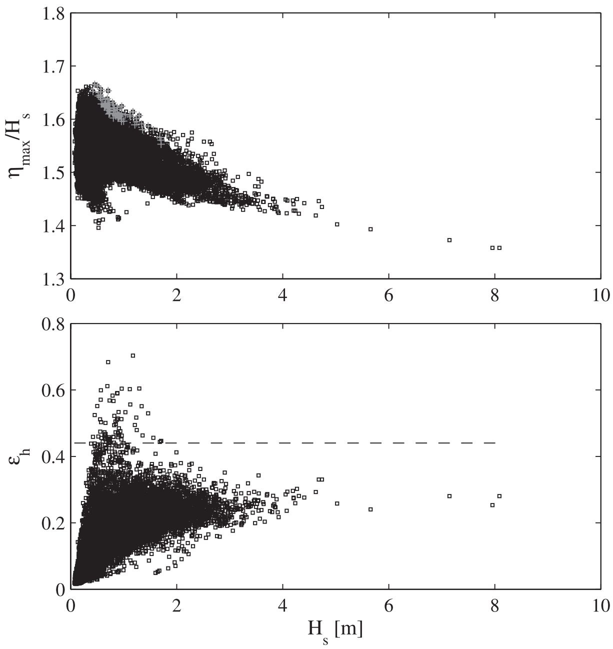

FIG. 7. NOAA buoy 42003 (east Gulf): (top) short-term expected maximum surface height $\eta_{\max}$ over an area $E_s = L^2$ ($L = 10^3$ m) for each hourly sea state (period 2007–09) in terms of the ratio $\eta_{\max}/H_s$, with H_s being the significant wave height, and (bottom) steepness ε_h of the associated extreme wave (dashed line is the Stokes–Miche upper limit). The wave dimension β is ~3 for all the analyzed sea states.

The present EPS model provides another ''hand on the elephant'' for the subject of extreme waves (see, e.g., Boccotti 1981, 2000; Fedele 2008; Fedele and Tayfun 2009; Gemmrich and Garrett 2008) by demonstrating that the occurrence of large waves over an area can be explained in terms of extremes in space–time. In particular, the proposed model is of relevance as a practical tool for identifying safer shipping routes and for improving the design and safety of offshore facilities.

The correlation or stochastic dependence of wave extremes is not an issue for the statistics of maxima because realizations of maxima typically occur at times and locations typically well separated to render them largely independent of one another in wind seas. However, under conditions conducive to the rapid development of long-crested sea states such as those studied numerically by Waseda et al. (2011), stochastic dependence can be an important factor in analysis. In this regard, the space–time stochastic model proposed here can be extended to smoothly bridge long- and short-crested conditions by taking into account the correlation between neighboring waves (see, e.g., Fedele 2005).

APPENDIX A

Wave Parameters

Drawing from Baxevani and Richlik (2004), the mean period and wavelengths are given by

$$\overline{T} = 2\pi\sqrt{\frac{m_{000}}{m_{002}}}, \quad \overline{L_x} = 2\pi\sqrt{\frac{m_{000}}{m_{200}}}, \quad \text{and}$$
$$\overline{L_y} = 2\pi\sqrt{\frac{m_{000}}{m_{020}}}. \tag{A1}$$

Here,

$$m_{ijk} = \int\int k_x^i k_y^j \omega^k W(\omega, \theta)\, d\omega\, d\theta \tag{A2}$$

are spectral moments of the directional spectrum W.

In (21) and (22), the coefficients N_S and N_V are given by

$$N_V = 2\pi\frac{XY}{\overline{L_x}\,\overline{L_y}}\alpha_{xyt} \quad \text{and} \tag{A3}$$

$$N_S = \sqrt{2\pi}\left(\frac{X}{\overline{L_x}}\sqrt{1-\alpha_{xt}^2} + \frac{Y}{\overline{L_y}}\sqrt{1-\alpha_{yt}^2}\right), \tag{A4}$$

with

$$\alpha_{xyt} = \sqrt{1 - \alpha_{xt}^2 - \alpha_{yt}^2 - \alpha_{xy}^2 + 2\alpha_{xy}\alpha_{xt}\alpha_{yt}}, \tag{A5}$$

where

$$\alpha_{xt} = \frac{m_{101}}{\sqrt{m_{200}m_{002}}}, \quad \alpha_{yt} = \frac{m_{011}}{\sqrt{m_{020}m_{002}}}, \quad \text{and}$$
$$\alpha_{xy} = \frac{m_{110}}{\sqrt{m_{200}m_{020}}}. \tag{A6}$$

APPENDIX B

Scale Dimension of Extremes

Consider the maximum wave surface height $\eta_{\max}$ over Ω. From the associated probability of exceedance (15), the expected value $\overline{\eta}_{\max}$ is given, according to the theory of extremes (Gumbel 1958), by

$$\frac{\overline{\eta}_{\max}}{H_s} = \zeta_0 + \frac{\gamma_e}{16\zeta_0 - \dfrac{F'(\zeta_0)}{F(\zeta_0)}}, \tag{B1}$$

where $\gamma_e = 0.5772$ is the Euler–Mascaroni constant; the prime denotes derivative with respect to $\zeta = z/H_s$; and the dimensionless ζ_0 satisfies

$$F(\zeta)\exp(-8\zeta^2) = 1, \tag{B2}$$

with

$$F(\zeta) = 16M_3\zeta^2 + 4M_2\zeta + M_1. \tag{B3}$$

Consider now as a reference the order statistics of N waves whose parent distribution follows an exceedance distribution of the form

$$P(\eta \mid H_s > z) = (4\zeta)^{\beta-1}\exp(-8\zeta^2), \tag{B4}$$

where the parameter $\beta \geq 1$. In particular, for $\beta = 1$ (B4) reduces to the Rayleigh law (7) for 1D waves and for $\beta =$ 2 and 3 to the distributions P_S and P_V in (7) and (8) for 2D and 3D waves, respectively. Thus, β is interpreted as a scale dimension of waves: that is, the relative scale of the wave with respect to the volume's size.

In the following, β is related to the mean wavelengths and periods as well as the volume's geometry by equating the expected maximum $\overline{\eta}_\beta$ of N "beta waves" to the true maximum $\overline{\eta}_{\max}$ in (B1). Indeed, from (B4) according to the theory of extremes (Gumbel 1958) the expected maximum $\overline{\eta}_\beta$ of N beta waves is given by

$$\frac{\overline{\eta}_\beta}{H_s} = \zeta_N + \frac{\gamma_e}{16\zeta_N - \beta/\zeta_N}, \tag{B5}$$

where, from (B4), ζ_N satisfies $N(4\zeta)^\beta\exp(-8\zeta^2) = 1$. The two expected maxima $\overline{\eta}_\beta$ and $\eta_{\max}$ are identical if β and N are chosen as

$$\beta = 1 + \zeta_0\frac{F'(\zeta_0)}{F'(\zeta_0)} = 3 - \frac{4M_2\zeta_0 + 2M_1}{16M_3\zeta_0^2 + 4M_2\zeta_0 + M_1} \tag{B6}$$

and

$$N = \frac{F(\zeta_0)}{4\zeta_0} = 4M_3\zeta_0 + M_2 + \frac{M_1}{4\zeta_0}, \tag{B7}$$

respectively. Here, N is the average number of waves of dimension β that occur within Ω.

APPENDIX C

Derivation of $\Pr\{\eta_{\max} > z \mid \Omega\}$

In (18), assume the stochastic independence of the events $\{\eta_{\max} \leq z \mid V\}$, $\{\eta_{\max} \leq z \mid S_L\}$, $\{\eta_{\max} \leq z \mid \partial S_L\}$, $\{\eta_{\max} \leq z \mid S_b\}$, and $\{\eta_{\max} \leq z \mid S_u\}$ (valid for large z). Then, the probability of exceedance can be rewritten as

$$\begin{aligned}\Pr\{\eta_{\max} > z \mid \Omega\} = 1 - \Pr\{\eta_{\max} \leq z \mid V\} \\ \cdot \Pr\{\eta_{\max} \leq z \mid S_L\} \cdot \Pr\{\eta_{\max} \leq z \mid \partial S_L\} \\ \cdot \Pr\{\eta_{\max} \leq z \mid S_b\} \cdot \Pr\{\eta_{\max} \leq z \mid S_u\}.\end{aligned} \tag{C1}$$

Further, the last two terms on the right-hand side can be set equal to 1, assuming that the significant wave height is null or small in the beginning and at the end of the storm [$M_{2,h} = 0$ in (9)]. This simplifies (C1) to

$$\begin{aligned}\Pr\{\eta_{\max} > z \mid \Omega\} = 1 - \Pr\{\eta_{\max} \leq z \mid V\} \\ \cdot \Pr\{\eta_{\max} \leq z \mid S_L\} \\ \cdot \Pr\{\eta_{\max} \leq z \mid \partial S_L\}.\end{aligned} \tag{C2}$$

Here, the terms on the right-hand side can now be formulated a la Borgman as in (12)–(14) assuming the stochastic independence of the sea-state events: namely,

$$\begin{aligned}&A_j = \{\eta_{\max} \leq z \mid \Delta V_j\}, \quad B_j = \{\eta_{\max} \leq z \mid \Delta S_j\}, \\ &C_j = \{\eta_{\max} \leq z \mid \partial\Delta S_j\}.\end{aligned} \tag{C3}$$

As a result,

$$\begin{aligned}\Pr\{\eta_{\max} \leq z \mid V\} &= \Pr\Big\{\bigcap_{j=1,J} A_j\Big\} \\ &= \prod_{j=1}^{J}[1 - P_V(z_1 \mid H_s = h_j)]^{M_3(\Delta t, X, Y \mid H_s = h_j)},\end{aligned} \tag{C4}$$

$$\begin{aligned}\Pr\{\eta_{\max} \leq z \mid S_L\} &= \Pr\Big\{\bigcap_{j=1,J} B_j\Big\} \\ &= \prod_{j=1}^{J}[1 - P_S(z_1 \mid H_s = h_j)]^{M_{2,v}(\Delta t, X, Y \mid H_s = h_j)},\end{aligned} \tag{C5}$$

and

$$\begin{aligned}\Pr\{\eta_{\max} \leq z \mid \partial S_L\} &= \Pr\Big\{\bigcap_{j=1,J} C_j\Big\} \\ &= \prod_{j=1}^{J}[1 - P(z_1 \mid H_s = h_j)]^{M_1(\Delta t, 0, 0, \mid H_s = h_j)},\end{aligned} \tag{C6}$$

where $h_j = h(t_j)$, and P_V, P_S, and P follow from (6), (8), and (7) as the probabilities that a 3D, 2D, and 1D wave has an amplitude larger than z in ΔV_j, in ΔS_j, and along its perimeter $\partial \Delta S_j$, respectively (see Fig. 1). The linear amplitude z_1 is related to the nonlinear amplitude z via the quadratic equation $z = z_1 + \mu z_1^2/2\sigma$, where μ is an integral measure of steepness (Tayfun 1980; Fedele and Tayfun 2009). Taking the limit of $\Delta t \to 0$ or $J \to \infty$ in (C3)–(C6) yields the extended Borgman exceedance probability (19) to space–time.

APPENDIX D

Function $G(\lambda, a)$

$$G(\lambda, a) = \begin{cases} \dfrac{\sin(\pi/\lambda)}{\pi/\lambda} \displaystyle\int_1^\infty \left.\frac{d^2P}{dz^2}\right|_{ax} (x-1)^{-1/\lambda}\, dx, & \lambda > 1 \\ \dfrac{d^2P}{da^2}, & \lambda = 1 \\ \dfrac{(-1)^n a^n}{n!} \dfrac{\sin(\pi\xi)}{\pi\xi} \displaystyle\int_1^\infty \left.\frac{d^{n+2}P}{dz^{n+2}}\right|_{ax} (x-1)^{-\mu}\, dx, & \lambda = \dfrac{1}{n+\xi} < 1, \end{cases} \tag{D1}$$

with (integer) $n > 1$ and $0 < \xi < 1$. If $\lambda = 1/n$ is rational (i.e., $\xi = 0$), then, from (D1),

$$G(\lambda, a) = -\frac{(-1)^n a^n}{n!} \frac{d^{n+1}P}{da^{n+1}}. \tag{D2}$$

REFERENCES

Adler, R. J., 1981: *The Geometry of Random Fields.* John Wiley, 275 pp.

——, 2000: On excursion sets, tube formulae, and maxima of random fields. *Ann. Appl. Probab.,* **10,** 1–74.

——, and J. E. Taylor, 2007: *Random Fields and Geometry. Springer Monogr. in Mathematics,* Vol. 115, Springer, 454 pp.

Allender, J., and Coauthors, 1989: The WADIC project: A comprehensive field evaluation of directional wave instrumentation. *Ocean Eng.,* **16,** 505–536.

Arena, F., 2004: On the prediction of extreme sea waves. *Environmental Sciences and Environmental Computing,* Vol. 2, P. Zannetti, Ed., EnviroComp Institute, CD-ROM.

——, and D. Pavone, 2006: The return period of non-linear high wave crests. *J. Geophys. Res.,* **111,** C08004, doi:10.1029/2005JC003407.

——, and ——, 2009: A generalized approach for the long-term modelling of extreme sea waves. *Ocean Modell.,* **26,** 217–225.

Baxevani, A., and I. Richlik, 2004: Maxima for Gaussian seas. *Ocean Eng.,* **33,** 895–911.

Bechle, A. J., and C. H. Wu, 2011: Virtual wave gauges based upon stereo imaging for measuring surface wave characteristics. *Coastal Eng.,* **58,** 305–316.

Benetazzo, A., 2006: Measurements of short water waves using stereo matched image sequences. *Coastal Eng.,* **53,** 1013–1032.

——, F. Fedele, G. Gallego, P.-C. Shih, and A. Yezzi, 2012: Offshore stereo measurements of gravity waves. *Coastal Eng.,* **64,** 127–138.

Boccotti, P., 1981: On the highest waves in a stationary Gaussian process. *Atti Accad. Ligure Sci. Lett.,* **38,** 271–302.

——, 1997a: A general theory of three-dimensional wave groups. Part I: The formal derivation. *Ocean Eng.,* **24,** 265–280.

——, 1997b: A general theory of three-dimensional wave groups. Part II: Interaction with a breakwater. *Ocean Eng.,* **24,** 281–300.

——, 2000: *Wave Mechanics for Ocean Engineering.* Elsevier, 496 pp.

Borgman, L. E., 1973: Probabilities for the highest wave in a hurricane. *J. Waterw. Port Coastal Ocean Eng. Div.,* **99,** 185–207.

Dankert, H., J. Horstmann, S. Lehner, and W. G. Rosenthal, 2003: Detection of wave groups in SAR images and radar image sequences. *IEEE Trans. Geosci. Remote Sens.,* **41,** 1437–1446.

de Vries, S., D. F. Hill, M. A. de Schipper, and M. J. F. Stive, 2011: Remote sensing of surf zone waves using stereo imaging. *Coastal Eng.,* **58,** 239–250.

Fedele, F., 2005: Successive wave crests in Gaussian seas. *Probab. Eng. Mech.,* **20,** 355–363.

——, 2008: Rogue waves in oceanic turbulence. *Physica D,* **237** (14–17), 2127–2131.

——, and M. A. Tayfun, 2009: On nonlinear wave groups and crest statistics. *J. Fluid Mech.,* **620,** 221–239.

——, and F. Arena, 2010: Long-term statistics and extreme waves of sea storms. *J. Phys. Oceanogr.,* **40,** 1106–1117.

——, Z. Cherneva, M. A. Tayfun, and C. Guedes Soares, 2010: NLS invariants and nonlinear wave statistics. *Phys. Fluids,* **22,** 036601, doi:10.1063/1.3325585.

——, A. Benetazzo, and G. Z. Forristall, 2011a: Space-time waves and spectra in the northern Adriatic Sea via a wave acquisition stereo system. *Proc. 30th Int. Conf. on Offshore Mechanics and Arctic Engineering,* Rotterdam, Netherlands, ASME, OMAE2011-49924.

——, G. Gallego, A. Benetazzo, A. Yezzi, M. Sclavo, M. Bastianini, and L. Cavaleri, 2011b: Euler characteristics and maxima of oceanic sea states. *J. Math. Comput. Sim.,* **82,** 1102–1111.

Forristall, G. Z., 2006: Maximum wave heights over an area and the air gap problem. *Proc. 25th Int. Conf. Offshore Mechanics and Arctic Engineering,* Hamburg, Germany, ASME, OMAE2006-92022.

——, 2007: Wave crest heights and deck damage in Hurricanes Ivan, Katrina and Rita. *Proc. Offshore Technology Conf.,* Houston, TX, OTC 18620.

——, and K. C. Ewans, 1998: Worldwide measurements of directional wave spreading. *J. Atmos. Oceanic Technol.,* **15,** 440–469.

Gallego, G., A. Yezzi, F. Fedele, and A. Benetazzo, 2011: A variational stereo algorithm for the three-dimensional reconstruction of ocean waves. *IEEE Trans. Geosci. Remote Sens.,* **49,** 4445–4457.

Gemmrich, J. R., and C. Garrett, 2008: Unexpected waves. *J. Phys. Oceanogr.,* **38,** 2330–2336.

Goda, Y., 1999: *Random Seas and Design of Maritime Structures.* World Scientific, 443 pp.

Guedes Soares, C., 1988: Bayesian prediction of design wave height. *Proc. Second Working Conf. on Reliability and Optimization of Structural Systems,* London, United Kingdom, IFIP Working Group, 311–323.

Gumbel, E. J., 1958: *Statistics of Extremes.* Columbia University Press, 373 pp.

Isaacson, M., and N. G. Mackenzie, 1981: Long-term distributions of ocean waves: A review. *J. Waterw. Port Coastal Ocean Div.,* **107,** 93–109.

Janssen, P. A. E. M., 2003: Nonlinear four-wave interactions and freak waves. *J. Phys. Oceanogr.,* **33,** 863–884.

Krogstad, H. E., 1985: Height and period distributions of extreme waves. *Appl. Ocean Res.,* **7,** 158–165.

Marom, M., R. M. Goldstein, E. B. Thornton, and L. Shemer, 1990: Remote sensing of ocean wave spectra by interferometric synthetic aperture radar. *Nature,* **345,** 793–795.

——, L. Shemer, and E. B. Thornton, 1991: Energy density directional spectra of nearshore wavefield measured by interferometric synthetic aperture radar. *J. Geophys. Res.,* **96,** 22 125–22 134.

Michell, J. H., 1893: On the highest waves in water. *Philos. Mag.,* **5,** 430–437.

Mori, N., and P. A. E. M. Janssen, 2006: On kurtosis and occurrence probability of freak waves. *J. Phys. Oceanogr.,* **36,** 1471–1483.

O'Reilly, W. C., T. H. C. Herbers, R. J. Seymour, and R. T. Guza, 1996: A comparison of directional buoy and fixed platform measurements of Pacific swell. *J. Atmos. Oceanic Technol.,* **13,** 231–238.

Piterbarg, V., 1995: *Asymptotic Methods in the Theory of Gaussian Processes and Fields. Translations of Mathematical Monographs,* Vol. 148, American Mathematical Society, 206 pp.

Prevosto, M., H. E. Krogstad, and A. Robin, 2000: Probability distributions for maximum wave and crest heights. *Coastal Eng.,* **40,** 329–360.

Rice, S. O., 1944: Mathematical analysis of random noise. *Bell Syst. Tech. J.,* **23,** 282–332.

——, 1945: Mathematical analysis of random noise. *Bell Syst. Tech. J.,* **24,** 46–156.

Rosenthal, W., and S. Lehner, 2008: Rogue waves: Results of the MaxWave project. *J. Offshore Mech. Arc. Eng.,* **130,** 021006, doi:10.1115/1.2918126.

Stokes, G. G., 1880: Considerations relative to the greatest height of oscillatory irrotational waves which can be propagated without change of form. *On the Theory of Oscillatory Waves,* G. G. Stokes, Ed., Cambridge University Press, 225–229.

Tamura, H., T. Waseda, and Y. Miyazawa, 2009: Freakish sea state and swell-windsea coupling: Numerical study of the *Suwa-Maru* incident. *Geophys. Res. Lett.,* **36,** L01607, doi:10.1029/2008GL036280.

Tayfun, M. A., 1979: Joint occurrences in coastal flooding. *J. Waterw. Port Coastal Ocean Div.,* **105,** 107–123.

——, 1980: Narrow band nonlinear sea waves. *J. Geophys. Res.,* **85** (C3), 1548–1552.

——, 1986: On narrow-band representation of ocean waves. 1. Theory. *J. Geophys. Res.,* **91** (C6), 7743–7752.

——, 2008: Distributions of envelope and phase in wind waves. *J. Phys. Oceanogr.,* **38,** 2784–2800.

——, and F. Fedele, 2007: Wave-height distributions and nonlinear effects. *Ocean Eng.,* **34** (11–12), 1631–1649.

Taylor, J., A. Takemura, and R. Adler, 2005: Validity of the expected Euler characteristic heuristic. *Ann. Probab.,* **33,** 1362–1396.

Wanek, J. M., and C. H. Wu, 2006: Automated trinocular stereo imaging system for three-dimensional surface wave measurements. *Ocean Eng.,* **33** (5–6), 723–747.

Waseda, T., M. Hallerstig, K. Ozaki, and H. Tomita, 2011: Enhanced freak wave occurrence with narrow directional spectrum in the North Sea. *Geophys. Res. Lett.,* **38,** L13605, doi:10.1029/2011GL047779.

Worsley, K. J., 1996: The geometry of random images. *Chance,* **9,** 27–40.